Changes of electrical resistivity of swine liver after occlusion and postmortem

Dieter Haemmerich, *Omer R Ozkan, **Jang-Zern Tsai, ***S Tyler Staelin, ****Supan Tungjitkusolmun, ***David M Mahvi, and John G Webster

Department of Biomedical Engineering, University of Wisconsin, 1415 Engineering Drive, Madison, WI 53706, USA

*Department of Electrical Engineering, University of Istanbul, Turkey.

**Department of Electrical and Computer Engineering, University of Wisconsin, 1415 Engineering Drive, Madison, WI 53706, USA

***Department of Surgery, University of Wisconsin, Madison, WI 53792, USA

**** Department of Electronics Engineering, King Mongkut's Institute of Technology Ladkrabang, Chalongkrung Rd., Ladkrabang, Bangkok, 10520, Thailand

John G. Webster is the corresponding author (e-mail: webster@engr.wisc.edu, tel 608-263-1574, fax 608-265-9239).

Key words: tissue resistivity, liver resistivity, radiofrequency, *post-mortem*, *in-vivo* resistivity, *in-vitro* resistivity, *ex-vivo* resistivity

Submitted to Medical & Biological Engineering & Computing

Supported by NIH Grant HL56143

1. ABSTRACT

We measured resistivity of swine liver tissue *in-vivo*, during induced ischemia and at postmortem to quantify associated changes in resistivity. We used plunge-electrodes, the four-terminal method and a computer-automated measurement system to acquire resistivity between 10 Hz and 1 MHz. We measured liver resistivity *in-vivo* in three animals at 11 locations. At 10 Hz, resistivity was 758 ± 170 Ω·cm. At 1 MHz the resistivity was 250 ± 40 Ω·cm. We measured the resistivity time course during the first 10 min after occluding liver blood supply in one animal. Resistivity increased steadily during occlusion. We measured change in resistivity of an excised tissue sample during the first 12 h after excision in one animal. Resistivity increased during the first 2 h by 53 % at 10 Hz and by 32% at 1 MHz. After 2 h resistivity decreased, probably due to membrane breakdown. We fitted the resistivity data to a ColeCole circle from which we estimated extracellular resistance (R_e), intracellular resistance (R_i) and cell membrane capacitance (C_m). R_e increased during the first 2 h by 95%, then decreased, suggesting increase in extracellular volume. C_m increased during the first 4 h by 40% possibly due to closure of membrane channels, then decreased, suggesting membrane breakdown. R_i stayed constant during the initial 6 h, then increased.

2. INTRODUCTION

Data on tissue resistivity of different mammals, tissue types and frequency ranges have been reported (Stoy et al., 1982; Gabriel et al., 1996; Stuchly and Stuchly, 1980; Rush et al., 1963; Steendijk et al., 1993; Duck, 1990; Geddes and Baker, 1967; Faes et al., 1999). However there are little data on the variation in tissue resistivity after death (Zheng et al., 1984; Swatland, 1980; Surowiec et al., 1985) and especially the comparison of *in-vivo* to *ex-vivo*

measurements. There are some very early data (Rajewsky, 1938; Schwan, 1954) that report negligible change of resistivity within the first 24 h after death. Heroux and Bourdages (1994). report changes in extracellular resistance (R_e), intracellular resistance (R_i) and cell membrane capacitance (C_m) for rat liver, rat cortex and rat gluteus while administering a toxic drug, and up to 10 h after animal death. Konishi et al. (1995) report changes in R_e, R_i and C_m of freshly extracted rat liver tissue at different incubation temperatures up to 6 h after tissue extraction. We measured swine liver resistivity *in-vivo* in three animals. We continued measurement after excision of a tissue sample in one animal for 12 h to examine the amount of resistivity change. For the first 12 h after excision we then calculated the parameters R_e, R_i and C_m of a three-element electric tissue model to examine causes of resistivity change. We measured resistivity during an occlusion experiment in one animal, where hepatic blood supply was stopped to determine changes in resistivity due to ischemic effects.

3. METHODS

We used three domestic pigs (30 to 40 kg) for the experiments. We obtained preapproval for all animal experiments from the Institutional Animal Care and Use Committee, University of Wisconsin, Madison. All procedures were performed with the animals under general *anesthesia*. Induction of *anesthesia* was achieved by using an *intramuscular* injection of tiletamine hydrochloride, zolazepam hydrochloride and xylazine hydrochloride. The animals were then intubated and maintained on inhaled halothane. Once adequate *anesthesia* was achieved, the *abdomen* was opened. The body temperature of the animals was 39 °C.

We used the four-terminal measurement method, which minimizes the effects of polarization impedance (Steendijk et al., 1993) and which has been widely used for resistivity measurements in mammalian tissue (Rush, 1963; Steendijk et al., 1993; Bragos et al., 1996). We used four-electrode, silver 0.38 mm diameter plunge electrodes with electrode spacing of 1.5 mm and depth of 4 mm. We used the same measurement circuit that we used in previous studies on heart resistivity measurements (Tsai et al., 2000). We calibrated the circuit and electrodes using 0.9% saline solution. The outputs of the differential amplifier and of the current-to-voltage converter were connected to a HP54600B digital oscilloscope. The input signal was generated using a HP33120A function generator. Both the oscilloscope and the function generator feature a RS232 serial port. We used an IBM-PC compatible computer for controlling the signal generator and automatically applying sinusoidal signals of frequencies from 100 Hz to 1 MHz using the RS232 interface. The oscilloscope reported the rms-values of the differential amplifier output and the current-to-voltage converter output to the computer. The program running on the PC for controlling the devices was written in Microsoft Visual Basic and entered the measured data together with the calculated resistivity values into a Microsoft Excel Sheet for further processing. One measurement cycle incorporating the gathering of data at seven different frequencies took 25 s.

All resistivity measurements described below were performed at 10 Hz, 100 Hz, 1 kHz, 10 kHz, 100 kHz, 500 kHz and 1 MHz. We measured three animals at 11 locations in all liver lobes ~1 h after start of the anesthetic preparation.

In one of the animals we performed vascular inflow occlusion of the hepatic artery and the portal vein while continuing resistivity measurements at a single location in the right upper lobe for 10 min. In another animal we resected a $8 \times 9 \times 2$ cm piece of the left upper

lobe before killing the animal. We performed resistivity measurements on the extracted liver tissue at 0.5, 2, 4, 8 and 12 h after excision. At each time point we acquired 4 data sets, which were then averaged. Temperature of the tissue sample was recorded at the time points when data were acquired, and during the *in-vivo* measurements. Between the measurements at different time points, the probe was removed from the tissue and cleaned. Both the occlusion experiment and the *post-mortem* experiment were performed after finishing initial *in-vivo* measurements. All measurement locations were selected so that the tissue was thicker than 2 cm to reduce any errors from too thin tissue samples.

Biological tissue can be described by a three-element circuit model (see Figure 1) consisting of extracellular resistance (R_e), intracellular resistance (R_i) and cell membrane capacitance (C_m). We determined a least-square circle approximation (i.e. approximation to the ColeCole half-circle) of the resistivity data we acquired from the measurements on extracted liver tissue. From the circular approximation, we determined R_e, R_i and C_m as previously done by Konishi et al. (1995). We determined R_0 (dc) and R_∞ ($f \to \infty$) where the half-circle crossed the real axis and ω_{max}, where the half-circle had its maximal imaginary value (see Figure 2). We then estimated R_e, R_i and C_m according to:

$$R_e = R_0$$

$$R_i = \frac{R_0 \cdot R_\infty}{R_0 - R_\infty}$$

$$C_m = \frac{1}{\omega_{max} \cdot (R_e + R_i)}$$

We determined these parameters for *in-vivo* resistance (baseline value) and for all time points where we measured *ex-vivo* resistivity on the extracted liver sample.

4. RESULTS

First, we measured resistivity at 11 locations *in-vivo* in three animals. Then we performed the occlusion experiment on one animal, and measured resistivity time course of an extracted tissue sample of the second animal. Figure 3 shows the mean and standard deviation of 11 *in-vivo* measurements in three animals. Figure 4 shows the time course of resistivity during the occlusion experiment. Each data point is taken from only a single measurement due to time constraints. Figure 5 shows the time course of resistivity of the extracted tissue sample for the first 12 h after extraction. Each data point represents the average of four measurements. The initial value at $t = 0$ is from an *in-vivo* measurement at the location of tissue extraction. Figure 6 shows the time course of temperature of the extracted tissue sample. Figure 7 shows the time course of fitted parameters R_e, R_i and C_m of the extracted tissue sample in relation to baseline values (*in-vivo*, i.e. $t = 0$).

5. DISCUSSION

Figure 3 shows the mean and standard deviation of 11 *in-vivo* liver resistivity measurements, performed on 3 different animals. The standard deviation is higher at low frequencies. The liver is a very heterogenous organ, particularly in regards to distribution of blood vessels. Both number and size vary greatly depending upon location, which results in differences in local blood circulation. Blood has a resistivity of 100 to 200 Ω·cm (Gabriel et al., 1996;

Duck, 1990; Geddes and Baker, 1967) within the frequency range of 100 Hz to 1 MHz. At frequencies below 10 kHz the average measured values for liver resistivity are 700 to 800 Ω·cm. The difference compared to the resistivity of blood is much higher than at high frequencies. Therefore the amount of blood flow at the measurement site has a higher impact at low frequencies compared to high frequencies and results in greater variation of the acquired values. Figure 5 shows that resistivity increases for all frequencies from 0 to 2 h after removal of the liver. The difference is lowest at radio frequencies (e.g. +33% at 500 kHz) and increases for low frequencies (+184% at 1 kHz). One contribution to the rise in resistivity after excision is due to the temperature dependence of liver tissue. The conductivity temperature coefficient is highest at low frequencies where it ranges between 1%/°C and 2%/°C (Gabriel, 1996) and lies at about 1%/°C below temperatures of 50 °C at radio frequencies (Dadd et al., 1996). Assuming a resistivity temperature coefficient –1.5%/°C for frequencies above 1 kHz, we can estimate change of resistivity caused by temperature according to Figure 6 to be around 18% at the 0.5 h time point, and around 26% at the 2 h and later time points, compared to in-vivo values. The change in resistivity seen at the 0.5 h time point (e.g. 85% at 1 kHz, and 30% at 500 kHz) is therefore partially a result of the lower temperature. However, the rise in resistivity within the first 2 h is much higher than can be explained by a change in temperature alone. Later than 2 h after excision, the temperature stays between 20 °C and 22 °C, so all changes seen after that time stem from different effects. A large contribution to the initial resistivity increase most probably stems from ischemic effects, which was demonstrated by the occlusion experiment. The liver is more susceptible to ischemia than any other organ except the brain. Functional abnormality occurs 15 min after complete stoppage of blood flow into the liver (Bassi and Bernelli-

Zazzera, 1964; Delmas-Beauvieux et al., 1992). Figure 4 shows that resistivity rises significantly within the first minutes after blood supply has been stopped (e.g. +62% at 1 kHz and +24% at 500 kHz). Bragos et al. (1996) obtained similar results during resistivity measurement on the heart while obstructing a coronary artery. It is well known that metabolism and ATP concentration decline rapidly when blood supply is cut off. This results in reduced activity of the ion pumps, which leads to changes in ion distribution between inter- and extracellular spaces. More specifically, cessation of sodiumpotassium pump activity (Na^+-K^+-ATPase) leads to depolarization of the cell. Eventually the result is inflow of water and sodium, which causes cell swelling (Lambotte, 1986). Furthermore, influx of Ca^{2+} leads to swelling and rupture of mitochondria and to damage of the other organelles. Lysosomal enzymes are released within the cell finally resulting in cell death (Farber et al., 1981). Another contribution to the rise in resistivity may come from drainage of blood, since blood has a much lower resistivity compared to liver tissue as discussed earlier.

We see the same initial rise in resistivity in the measurements of extracted liver tissue. Figure 5 shows that this initial rise persisted until 2 h postmortem. Considering the electric tissue model from Figure 1, this rise is mainly due to increase in extracellular resistance as seen in Figure 7. The rise in extracellular resistance is the result of a decline in extracellular fluid volume. The membrane capacity C_m also rises initially and reaches its peak 4 h postmortem. This membrane capacitance rises due to the increase in membrane surface resulting from cell swelling. Other contributions might come from the closure of membrane ion channels due to ATP depletion and depolarization, and from closure of gap junctions. Gap junctions represent a path between neighboring cells that allow the passage of molecules smaller than 1000 Da, particularly ions (Kumar and Gilula, 1996). In normal liver

parenchyma, each cell has an average of 6 neighboring cells. Gap junctions provide intercellular connections between all neighboring cells (Meyer et al., 1981). Schellens et al. (1987) found initial changes in the structural arrangement of Connexin 32, the protein that forms gap junctions in the liver, 30 min after induced ischemia *in-vivo*. Meyer et al. (1981) observed that the intercellular resistivity ρ_i increases from ~3000 Ω·cm in normal liver to ~30000 Ω·cm in regenerating liver, where only few gap junctions are present. Closure of gap junctions might contribute to the steady rise of resistivity within the first 2 h.

After 2 h postmortem, resistivity decreases. Several factors may contribute to this decrease. Heffron and Hegarty (1974) found an increase in extracellular fluid due to loss of membrane integrity *postmortem*, which allows continuity between intracellular and extracellular fluid compartments. As discussed earlier, lysosomal agents are released within the cell contributing to cell membrane damage. Figure 7 shows that the resistivity decrease is accompanied by a decrease of both extracellular resistance R_e and membrane capacitance C_m. The decrease in R_e is in agreement with the increase in extracellular fluid volume. After tissue suffers extensive postmortem damage, cell membranes begin to break down (Swatland, 1980). The loss of membrane integrity results in a steady decrease in membrane capacitance. Astbury et al. (1988) observed decrease in low-frequency resistivity of canine spleen within 10 h after death of the animal. These changes were accompanied by membrane breakdown, which they confirmed histologically. Membrane breakdown preferentially decreases the low-frequency resistivity, where magnitude of resistivity is mainly governed by existence of cell membranes that force the current (i.e. ions) to flow in extracellular fluid.

For the parameters R_e, R_i and C_m we acquired results similar to those of Konishi et al. (1995). During their *ex-vivo* measurements at 20 °C they observed initial rises of R_e and C_m with peaks 1.5 h post-mortem, followed by steady decreases.

Our results show that there is significant change of tissue resistivity after removal of the organ and that accurate results require *in-vivo* measurements with intact circulation.

6. REFERENCES

ASTBURY, J. C., GOLDSCHMIDT, M. H., EVANS, S., NEIBAUER, G. W., FOSTER, K. R., 'The dielectric properties of canine normal and neoplastic splenic tissues', *Proc. 14th Northeast Bioeng. Conf.*, Durham, NH, March 1988.

BASSI, M., BERNELLI-ZAZZERA, A. (1964), 'Ultrastructural cytoplasmic changes of liver cells after reversible and irreversible ischemia', *Exp. Mol. Pathol.*, **3**, pp. 332–350

BRAGÓS, R., RIU, P., WARREN, M., TRESÀNCHEZ, M., CARREÑO, A. and CINCA, J. (1996): 'Changes in myocardial impedance spectrum during acute ischemia in the in-situ pig heart', *Proc. 18th Annu. Int. Conf. IEEE Eng. Med. Biol. Soc*., Amsterdam, Paper number: 414

DADD, J. S., RYAN, T. P. and PLATT, R. (1996): 'Tissue impedance as a function of temperature and time', *Biomed. Sci. Instrum.*, **32**, pp. 205–214

DELMAS-BEAUVIEUX, M. C., GALLIS, J. L., ROUSSE, N., MICHEL, C. P. (1992), 'Phosphorus-31 nuclear magnetic resonance of isolated rat liver during hypothermic ischemia and subsequent normothermic perfusion', *J. Hepatol.*, **15**, pp. 192–201

DUCK, F. A. (1990): *Physical properties of tissue: a comprehensive reference book*, San Diego: Academic Press

FAES, T. J., VAN DER MEIJ, H. A., DE MUNCK, J. C., HEETHAAR, R. M. (1999): 'The electric resistivity of human tissues (100 Hz – 10 MHz): a meta-analysis of review studies', *Physiol. Meas.*, **20**, pp. R1–10

FARBER, J. L., CHIEN, K. R., MITTNACHT, S. JR. (1981), 'Myocardial ischemia: the pathogenesis of irreversible cell injury in ischemia', *Am. J. Pathol.*, **102**, pp. 271–281

GABRIEL, C., GABRIEL, S. and CORTHOUT, E. (1996): 'The dielectric properties of biological tissues: 1. literature survey', *Phys. Med. Biol.*, **41**, pp. 2231–2249

GEDDES, L.A. and BAKER, L. E. (1967): 'The specific resistance of biological material--a compendium of data for the biomedical engineer and physiologist', *Med. Biol. Eng.*, **5**, pp. 271–293

HEFFRON, J. J. and HEGARTY, P. V. (1974): 'Evidence for a relationship between atp hydrolysis and changes in extracellular space and fiber diameter during rigor development in skeletal muscle', *Comp. Biochem. Physiol.*, **49A**, pp. 43–56

HEROUX, P., BOURDAGES, M. (1994): 'Monitoring living tissues by electrical impedance spectroscopy', *Ann. Biomed. Eng.*, **22**, pp. 328–337

KONISHI, Y., MORIMOTO, T., KINOUCHI, Y., IRITANI, T., MONDEN, Y. (1995): 'Electrical properties of extracted rat liver tissue', *Res. Exp. Med.*, **195**, pp. 183–192

KUMAR, N. M. and GILULA, N. B. (1996): 'The gap junction communication channel', *Cell*, **84**, pp. 381–388

LAMBOTTE, L. (1986), 'Cellular swelling and anoxic injury of the liver', *Eur. Surg. Res.*, **18**, pp. 224–229

MEYER, D. J., YANCEY, S. B. and REVEL, J.P. (1981): 'Intercellular communication in normal and regenerating rat liver: a quantitative analysis', *J. Cell Biol.*, **91**, pp. 505–523

RAJEWSKY, B. (1938): *Ergebnisse der biphysikalischen Forschung*, **1**

RUSH, S., ABILDSKOV, J. A. and MCFEE, R. (1963): 'Resistivity of body tissues at low frequencies', *Circ. Res*., **12**, pp. 40–50

SCHELLENS, J. P. M., BLANGE, T. and GROOT, K. (1987): 'Gap junction ultrastructure in rat liver parenchymal cells after in vivo ischemia', *Virchow Arch. B*, **53**, pp. 347–352

SCHWAN, J. P. (1954): *Z. Naturforsch*, **96**, pp. 245–251

STEENDIJK, P., MUR, G., VAN DER VELDE, E. T. and BAAN, J. (1993): 'The four-electrode resistivity technique in anisotropic media: theoretical analysis and application on myocardial tissue in vivo', *IEEE Trans. Biomed. Eng*., **40**, pp. 138–148

STOY, R. D., FOSTER, K. R. and SCHWAN, H. P. (1982): 'Dielectric properties of mammalian tissues from 0.1 to 100 MHz: a summary of recent data', *Phys. Med. Biol.*, **27**, pp. 501–513

STUCHLY, M .A. and STUCHLY, S. S. (1980): 'Dielectric properties of biological substances – tabulated', *J. Microw. Power*, **15**, pp. 19–26

SUROWIEC, A., STUCHLY, S. S. and SWARUP, A. (1985): 'Radiofrequency dielectric properties of animal tissues as a function of time following death', *Phys. Med. Biol.*, **30**, pp. 1131–1141

SWATLAND, H. J. (1980): 'Postmortem changes in electrical capacitance and resistivity in pork', *J. Animal Sci.*, **51**, pp. 1108–1112

TSAI, J. Z., CAO, H., TUNGJITKUSOLMUN, S., WOO, E. J., VORPERIAN, V. R. and WEBSTER, J. G. (2000): 'Dependence of apparent resistance of four-electrode probes on insertion depth', *IEEE Trans. Biomed. Eng.*, **47**, pp. 41–48

ZHENG, E., SHAO, S. and WEBSTER, J. G. (1984): ‘Impedance of skeletal muscle from 1 Hz to 1 MHz’, *IEEE Trans. Biomed. Eng.*, **31**, pp. 477–480

7. FIGURE LEGENDS

Figure 1: Tissue equivalent circuit model.

Figure 2: ColeCole circle.

Figure 3: Resistivity decreases with frequency. Mean and standard deviation of 11 measurements in three animals.

Figure 4: Time course of resistivity during first 10 min after the blood vessels supplying the liver have been obstructed.

Figure 5: Time development of resistivity during first 12 h after excision of the liver. The leftmost value is the resistivity measured *in-vivo*.

Figure 6: Temperature of excised tissue sample during first 12 h after excision.

Figure 7: Change of extracellular resistance (R_e), intracellular resistance (R_i) and membrane capacitance (C_m) during first 12 h of excised tissue sample.

8. FIGURES

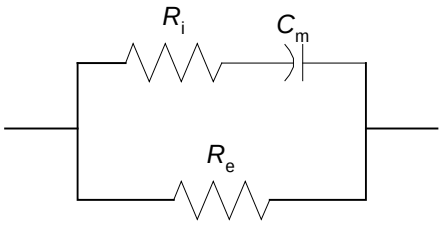

Figure 1: Tissue equivalent circuit model.

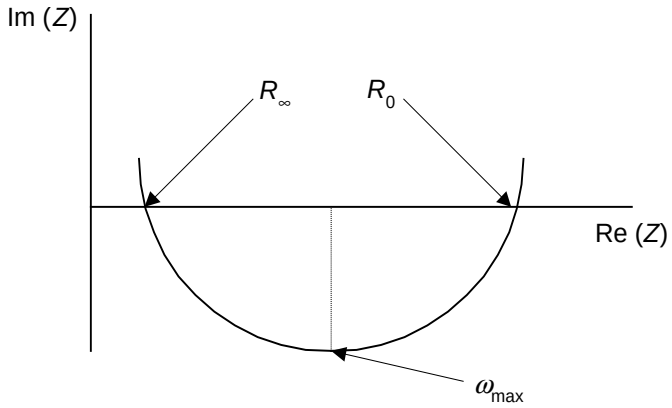

Figure 2: Cole–Cole circle.

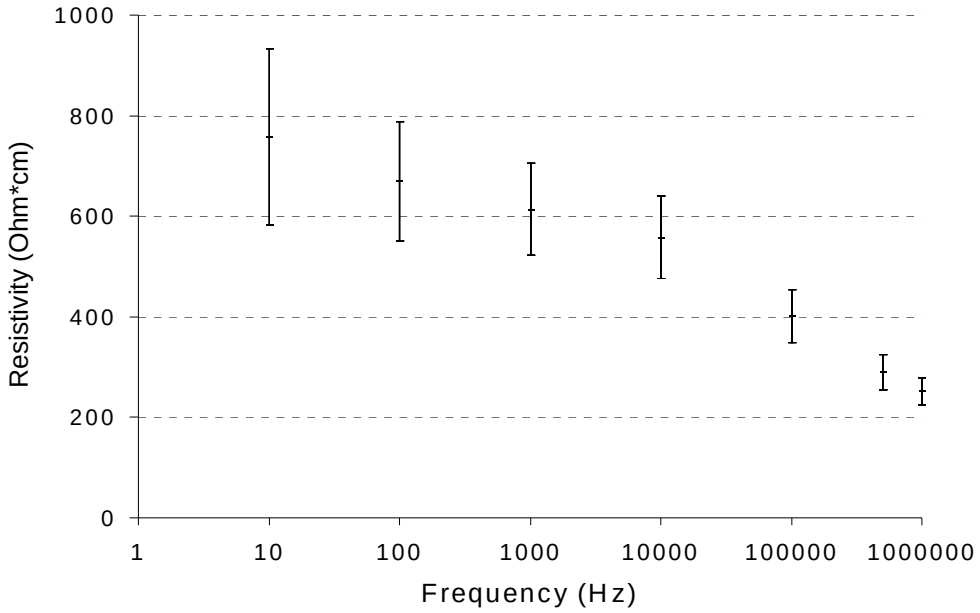

Figure 3: Resistivity decreases with frequency. Mean and standard deviation of 11 *in-vivo* measurements in three animals.

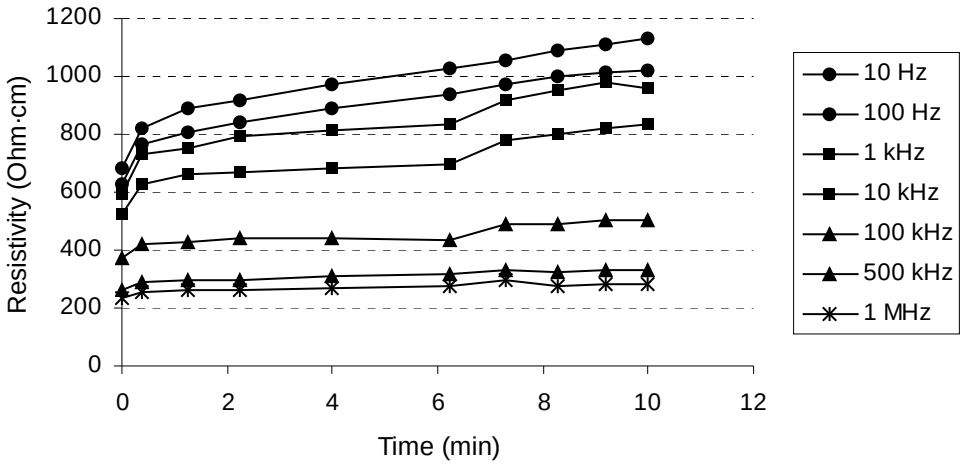

Figure 4: Time course of resistivity during first 10 min after the blood vessels supplying the liver have been obstructed.

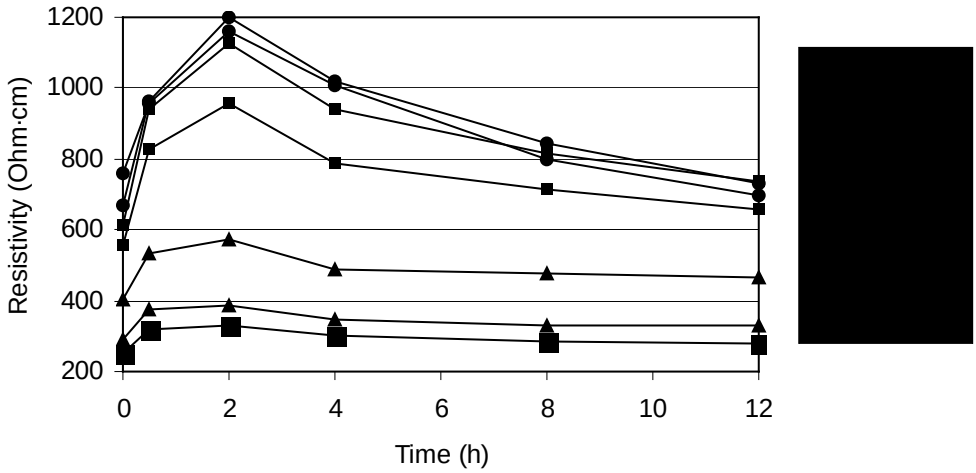

Figure 5: Time development of resistivity during first 12 h after excision of the liver.

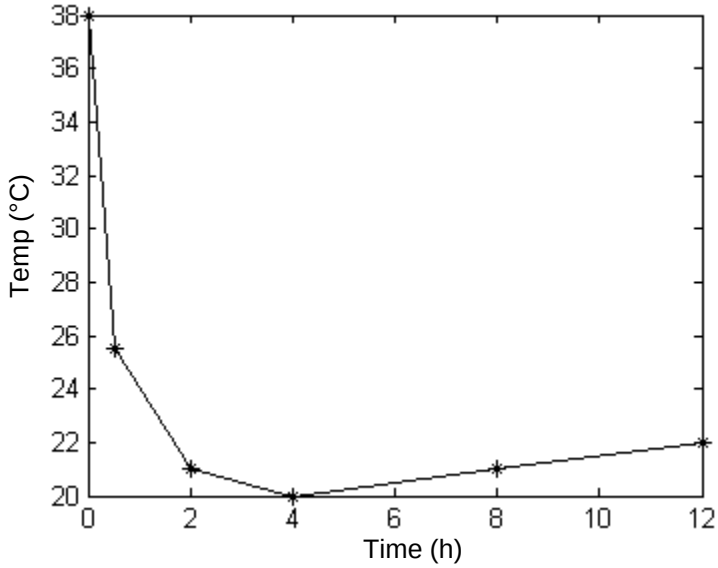

Figure 6: Temperature of excised tissue sample during first 12 h after excision.

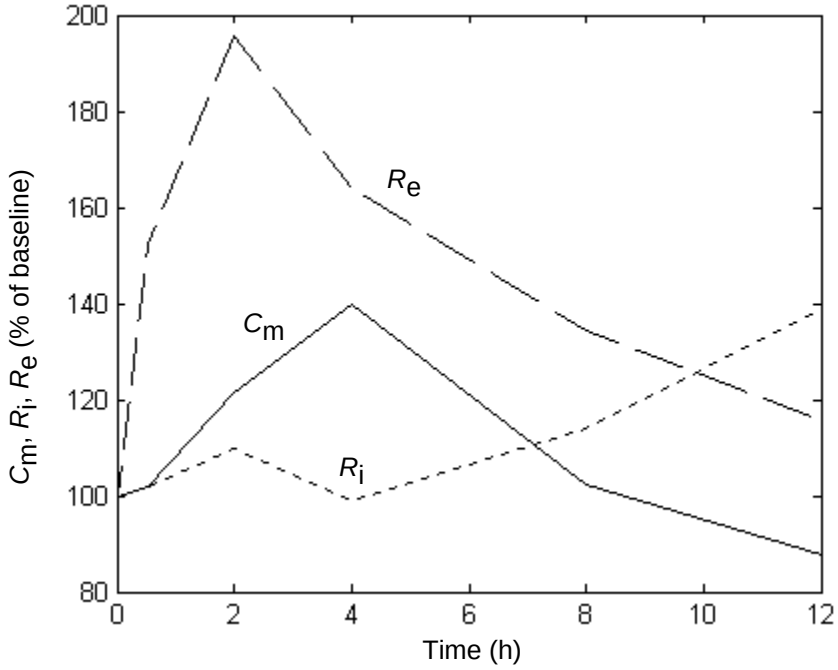

Figure 7: Change of extracellular resistance (R_e), intracellular resistance (R_i) and membrane capacitance (C_m) during first 12 h of excised tissue sample.